Supplementary Information

Dynamic behavior of an artificial protein needle contacting a membrane observed by high-speed atomic force microscopy

Takafumi Ueno,*[a] Kento Niwase,[a] Daisho Tsubokawa,[a] Kosuke Kikuchi,[a] Natsumi Takai,[b] Tadaomi Furuta,[a] Ryuji Kawano,[b] Takayuki Uchihashi[c,d]

[a] Department of Life Science and Technology, Tokyo Institute of Technology, Nagatsuta-cho, Midori-ku, Yokohama 226-8501, Japan

[b] Department of Biotechnology and Life Science, Tokyo University of Agriculture and Technology, 2-24-16 Naka-cho, Koganei, Tokyo 184-8588, Japan

[c]Department of Physics, Nagoya University, Nagoya, Aichi 464-8602, Japan

[d] Exploratory Research Center on Life and Living Systems (ExCELLS), National Institutes of Natural Sciences, Okazaki, Aichi 444-8787, Japan

Experiments

Materials. All reagents were purchased from commercial suppliers and used for experiments without further purification. Expression and purification of **PN** and **PN_ΔHis** were carried out as described previously.[1, 2] Lipid molecules were purchased from Avanti Polar Lipids, Inc. We used 10 mg/mL 1,2-dioleoyl-sn-glycero-3-phosphocholine (DOPC) chloroform solution. Liposomes were prepared by the sonication method.[3]

HS-AFM imaging. HS-AFM (Research Institute of Biomolecule Metrology Co. Ltd.; NanoExplore) measurements were made in the tapping mode. An amorphous carbon tip was produced on the original AFM tip (Olympus; BL-AC10DS) by electron-beam deposition and the tip was sharpened by plasma etching. HS-AFM imaging methods were performed as reported previously.[4, 5] The observations of **PN** were performed in a 20 mM Gly-HCl buffer (pH 3) containing 100 mM KCl at room temperature. Diluted protein samples (typically in a range between 10 to 50 nM **PN** concentration) were loaded onto freshly cleaved mica for 5 minutes and washed with 100 μL of 20 mM Gly-HCl buffer (pH 3.0, 100 mM KCl). The same procedure was performed for **PN_ΔHis**. The interaction between **PN** the and lipid bilayer was observed by the addition of **PN** to the mica modified with the lipid bilayer.[3] A 2 μL volume of a liposome solution containing 20 mM $MgCl_2$ was placed on mica, and allowed to stand at room temperature for 3 minutes. The membrane was then washed with 100 μL of ultrapure water to remove excess liposomes, and formation of a lipid bilayer membrane was confirmed. Next, 2 μL of buffer was removed from a buffer reservoir. Then 2 μL of a150 nM **PN** solution was added to a buffer reservoir (3 nM **PN** in a final concentration). Measurements were carried out at 5 or 10 frames per second. The same procedure was performed for **PN_ΔHis**.

Image analysis. A custom analysis program was used for processing of the HS-AFM data. The program was written in Python and used OpenCV as the image processing library.[6, 7] We constructed a system which recognizes **PN** and the lipid bilayer and collects data from the image after pretreatment including noise removal, a height correction, and automatic flattening. **PN** was approximated as an ellipse to determine the distance and angle between **PN** and the lipid bilayer. The distance was determined by calculating the shortest distance between the apex of the ellipse and the lipid bilayer. The angle was determined by calculating the inner product of the vector of the approximate line on the bilayer surface and the vector of the approximate major axis of the **PN** ellipse. Finally, the processed images were saved as time-series data grouped in single **PN** molecules. The analysis of $v_{\theta \mathbf{PN}}$ and $\theta_{\mathbf{PN}}$ was performed on 59 **PN** molecules for each set of conditions using the processed data. The same procedure was performed for 45 **PN_ΔHis** molecules.

Molecular dynamics simulations. A half model of **PN** (trimer) was prepared by complementing defect residues (N-terminal; E, C-terminal; TFLVEHHHHHH) of the structure (PDB ID 3A1M) reported by Yokoi (Figure S3).[2] Since the structures of the His-tag moieties could not be determined by crystal structure analysis of **PN**, an initial model of **PN** was obtained from a 5-ns MD simulation of **PN** in which a His-tag was linked to the C-terminal of foldon after equilibration (Figure S3). A DOPC membrane bilayer consisting of 512 molecules was created by doubling each molecule in the X and Y directions of a system containing 128 molecules equilibrated at 303 K (http://www.fos.su.se/~sasha/SLipids/Downloads.html). The obtained **PN** model was arranged vertically at a minimal distance of ~2 Å with the foldon tip oriented toward the lipid bilayer in systems arranged 90°, 45° and 0° from the Z-axis. TIP3P[8] was used to model water molecules and Na^+ was used as a counter ion in the system. Then, the **PN** model was moved at a rate of 10 nm/ns

and contacted with the lipid bilayer surface to provide **PN**–membrane structures which were subsequently used as initial structures. The **PN_ΔHis** model was prepared by removing HHHHHH from the C-terminus of the **PN** model. Systems reproducing the acidic conditions (pH 3.0) were prepared by protonating D, E, and H of the models according to p*K*a estimations based on PDB2PQR.[9] For each system, 5000-step energy minimization, 500-ps NVT equilibration, and 500-ps NPT equilibration were carried out with positional restraints on the heavy atoms of the **PN** model, and then a 50-ns production run without restraints was performed three times (with different initial velocities). Each of the MD simulations was performed using GROMACS version 4.6.5 and 2016.3.[10-16] Amber99SB-ildn[17] and Slipids[18, 19] force fields were used for proteins and DOPC lipids, respectively. The TIP3P[8] model was used for water molecules. The temperature and pressure were controlled using Nose-Hoover[20, 21] and Parrinello-Rahman[22] simulations (300 K and 1 bar). The electrostatic interactions were calculated using the particle mesh Ewald (PME) method.[23] The calculation of the van der Waals interactions was carried out with a cutoff distance of 1.0 nm. The angle of the **PN** model on the lipid bilayer was defined as the angle formed by the normal vector of the lipid bilayer and the direction vector from R83Cα to G12Cα of the **PN** model. Analysis of the number of hydrogen bonds was carried out with a cutoff radius of 0.38 nm and cutoff angle of 35°. The same procedure was performed for the **PN_ΔHis** model simulations.

Channel current conductance measurements. The bilayers were prepared using the droplet contact method.[24] Lipid bilayer membranes were formed in the micropores of the parylene film partitioning the two chambers of the droplet contact method device.[25-27] DOPC in *n*-decane (10 mg/mL) solution (2 μL) was added to two chambers and then they both were filled with PBS buffer (5 μL). A clean hydrophobic stick was then lightly dragged across the bilayer cup orifice to form a lipid bilayer. Bilayer formation was confirmed by continuous monitoring of the membrane

capacitance during the procedure and it reached 60-80 pF as indicated by formation of the thin bilayer. Signal current was monitored using a Pico2 amplifier (Tecella LLC, CA) tethered to an Ag/AgCl electrode in each chamber. The compartment connected to a grounded electrode is referred to as the *cis* side, and the compartment connected to the applied voltage electrode is referred to as the *trans* side. The **PN** solution in PBS buffer was injected into the *cis*-side chamber at a final concentration of 5 μM, and then electrical current data were acquired. The current data, with noise reduced using a 4 kHz of a low-pass filter, were acquired at a sampling frequency of 8 kHz. Analysis of the current signal was performed using Clampfit (Molecular Devices, Sunnyvale). To quantify the signal current, the charge flux J_Q ($pC \cdot s^{-1} \cdot cm^{-2}$) was calculated using three independent current recordings from each of the measurement conditions.[28, 29] The same procedure was performed for **PN_ΔHis**.

Quartz Crystal Microbalance (QCM). QCM measurements were performed on an AFFINIX Q4 system (INITIUM Inc.). The 27 MHz crystal with gold electrodes was washed with 1% SDS solution and 1:3 (v/v) H_2O_2/H_2SO_4 (piranha solution) before use. A DOPC vesicle (50 nm in diameter) solution was added to the cell to form a supported lipid bilayer on the surface of a clean gold electrode. Then **PN** solution was added and frequency change was monitored. A time-dependent change of the frequency was detected by the frequency meter to track the process of adsorption of **PN**. The same procedure was performed for **PN_ΔHis**.

Binding kinetics were analyzed using the time courses of frequency changes with the binding of **PN** to the lipid bilayer. The binding period after the injection is described by equations 1-3.

$$\Delta F = \Delta F_{t\to\infty}(1 - e^{-t/\tau}) \quad (1)$$

$$\frac{1}{\tau} = k_{on}[P]_0 + k_{off} \quad (2)$$

$$K_D = \frac{k_{off}}{k_{on}} \quad (3)$$

Where ΔF is the frequency change [Hz], $\Delta F_{t\to\infty}$ is a maximum frequency change [Hz], t is the measurement time [s], and τ is the relaxation time [s]. τ was calculated from the time course of ΔF at each concentration of **PN** ($[P]_0$) by a curve-fitting method based on eq 1. The k_{on} and k_{off} values were obtained from the slope and intercept of the linear correlation of the reciprocal plot of binding relaxation time ($1/\tau$) against each concentration of **PN** ($[P]_0$), using eq 2. K_D values were calculated from the obtained k_{on} and k_{off} values, using eq 3.

References

1. H. Inaba, N. J. M. Sanghamitra, K. Fujita, T. Sho, T. Kuchimaru, S. Kitagawa, S. Kizaka-Kondoh and T. Ueno, *Mol. Biosyst.*, 2015, **11**, 3111-3118.
2. N. Yokoi, H. Inaba, M. Terauchi, A. Z. Stieg, N. J. M. Sanghamitra, T. Koshiyama, K. Yutani, S. Kanamaru, F. Arisaka, T. Hikage, A. Suzuki, T. Yamane, J. K. Gimzewski, Y. Watanabe, S. Kitagawa and T. Ueno, *Small*, 2010, **6**, 1873-1879.
3. S. Morandat, S. Azouzi, E. Beauvais, A. Mastouri and K. El Kirat, *Anal. Bioanal. Chem.*, 2013, **405**, 1445-1461.
4. T. Uchihashi, N. Kodera and T. Ando, *Nat. Protoc.*, 2012, **7**, 1193-1206.
5. D. Yamamoto, T. Uchihashi, N. Kodera, H. Yamashita, S. Nishikori, T. Ogura, M. Shibata and T. Ando, in *Methods in Enzymology*, ed. N. G. Walter, Academic Press, 2010, vol. 475, pp. 541-564.
6. G. Bradski and A. Kaehler, *Learning OpenCV: Computer Vision with the OpenCV Library*, O'Reilly Media, Incorporated, 2008.
7. K. J. Millman and M. Aivazis, *Computing in Science Engineering*, 2011, **13**, 9-12.
8. W. L. Jorgensen, J. Chandrasekhar, J. D. Madura, R. W. Impey and M. L. Klein, *J. Chem. Phys.*, 1983, **79**, 926-935.
9. T. J. Dolinsky, P. Czodrowski, H. Li, J. E. Nielsen, J. H. Jensen, G. Klebe and N. A. Baker, *Nucleic Acids Res.*, 2007, **35**, W522-525.
10. H. J. C. Berendsen, D. van der Spoel and R. van Drunen, *Comput. Phys. Commun.*, 1995, **91**, 43-56.
11. E. Lindahl, B. Hess and D. van der Spoel, *Molecular modeling annual*, 2001, **7**, 306-317.
12. D. Van Der Spoel, E. Lindahl, B. Hess, G. Groenhof, A. E. Mark and H. J. C. Berendsen, *J. Comput. Chem.*, 2005, **26**, 1701-1718.
13. B. Hess, C. Kutzner, D. van der Spoel and E. Lindahl, *J. Chem. Theory Comput.*, 2008, **4**, 435-447.
14. S. Páll, M. J. Abraham, C. Kutzner, B. Hess and E. Lindahl, presented in part at the Solving Software Challenges for Exascale, 2015, 2015.
15. S. Pronk, S. Páll, R. Schulz, P. Larsson, P. Bjelkmar, R. Apostolov, M. R. Shirts, J. C. Smith, P. M. Kasson, D. van der Spoel, B. Hess and E. Lindahl, *Bioinformatics*, 2013, **29**, 845-854.
16. M. J. Abraham, T. Murtola, R. Schulz, S. Páll, J. C. Smith, B. Hess and E. Lindahl, *SoftwareX*, 2015, **1-2**, 19-25.
17. K. Lindorff-Larsen, S. Piana, K. Palmo, P. Maragakis, J. L. Klepeis, R. O. Dror and D. E. Shaw, *Proteins*, 2010, **78**, 1950-1958.
18. J. P. M. Jämbeck and A. P. Lyubartsev, *J. Chem. Theory Comput.*, 2012, **8**, 2938-2948.
19. J. P. M. Jämbeck and A. P. Lyubartsev, *J. Phys. Chem. B*, 2012, **116**, 3164-3179.
20. W. G. Hoover, *Phys. Rev. A*, 1985, **31**, 1695-1697.
21. S. Nosé, *Mol. Phys.*, 1984, **52**, 255-268.
22. M. Parrinello and A. Rahman, *J. Appl. Phys.*, 1981, **52**, 7182-7190.
23. T. Darden, D. York and L. Pedersen, *J. Chem. Phys.*, 1993, **98**, 10089-10092.
24. H. Watanabe and R. Kawano, *ANALYTICAL SCIENCES*, 2016, **32**, 57-60.
25. K. Funakoshi, H. Suzuki and S. Takeuchi, *Anal. Chem.*, 2006, **78**, 8169-8174.

26. Y. Tsuji, R. Kawano, T. Osaki, K. Kamiya, N. Miki and S. Takeuchi, *Lab Chip*, 2013, **13**, 1476-1481.
27. Y. Tsuji, R. Kawano, T. Osaki, K. Kamiya, N. Miki and S. Takeuchi, *Anal. Chem.*, 2013, **85**, 10913-10919.
28. H. Bayley, B. Cronin, A. Heron, M. A. Holden, W. L. Hwang, R. Syeda, J. Thompson and M. Wallace, *Mol. Biosyst.*, 2008, **4**, 1191-1208.
29. F. C. Macazo and R. J. White, *Anal. Chem.*, 2014, **86**, 5519-5525.

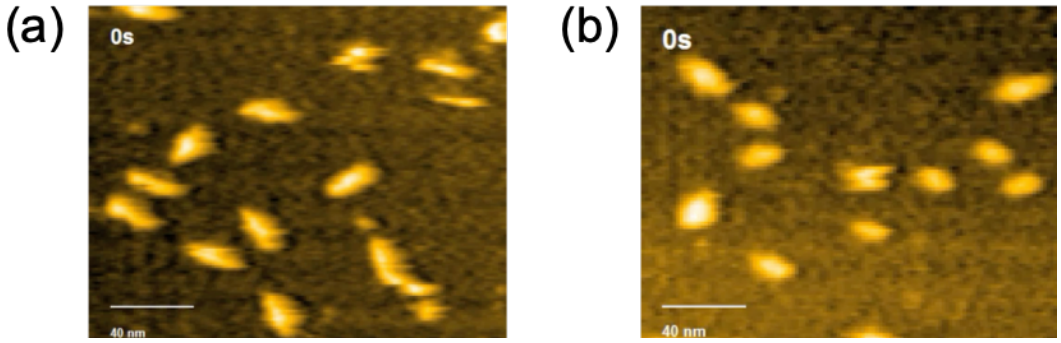

Fig. S1. HS-AFM images of **PN** (a) and **PN_ΔHis** (b) in a buffer solution of 20 mM Gly-HCl (pH 3) containing 100 mM KCl. Scale bar: 40 nm.

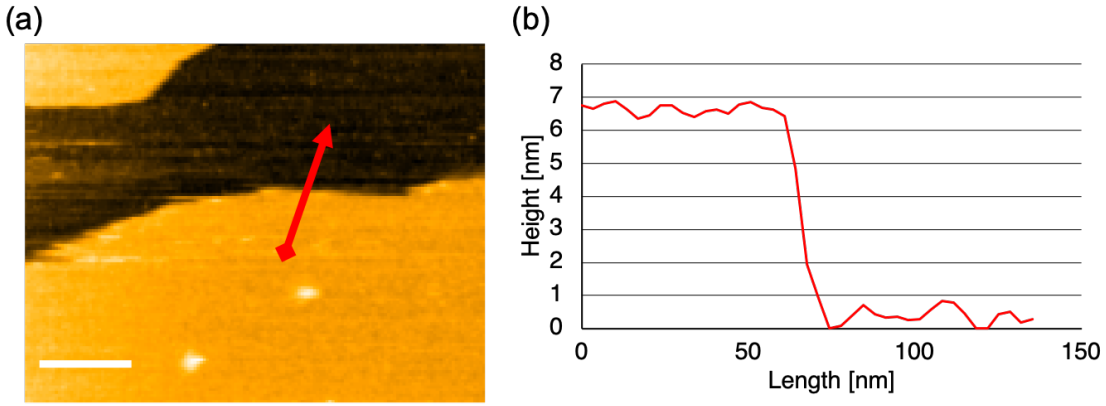

Fig. S2. HS-AFM image of the DOPC membrane (a) and the hight profile (b). Scale bar: 100 nm.

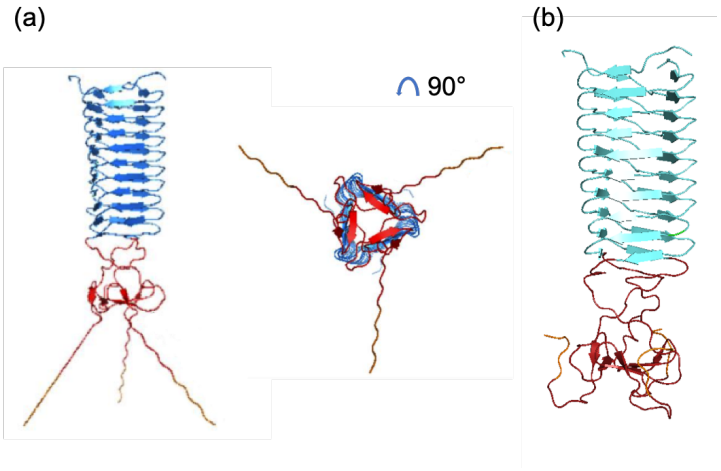

Fig. S3. Initial model of PN for MD simulation (a) and the structure after 5 ns production run.

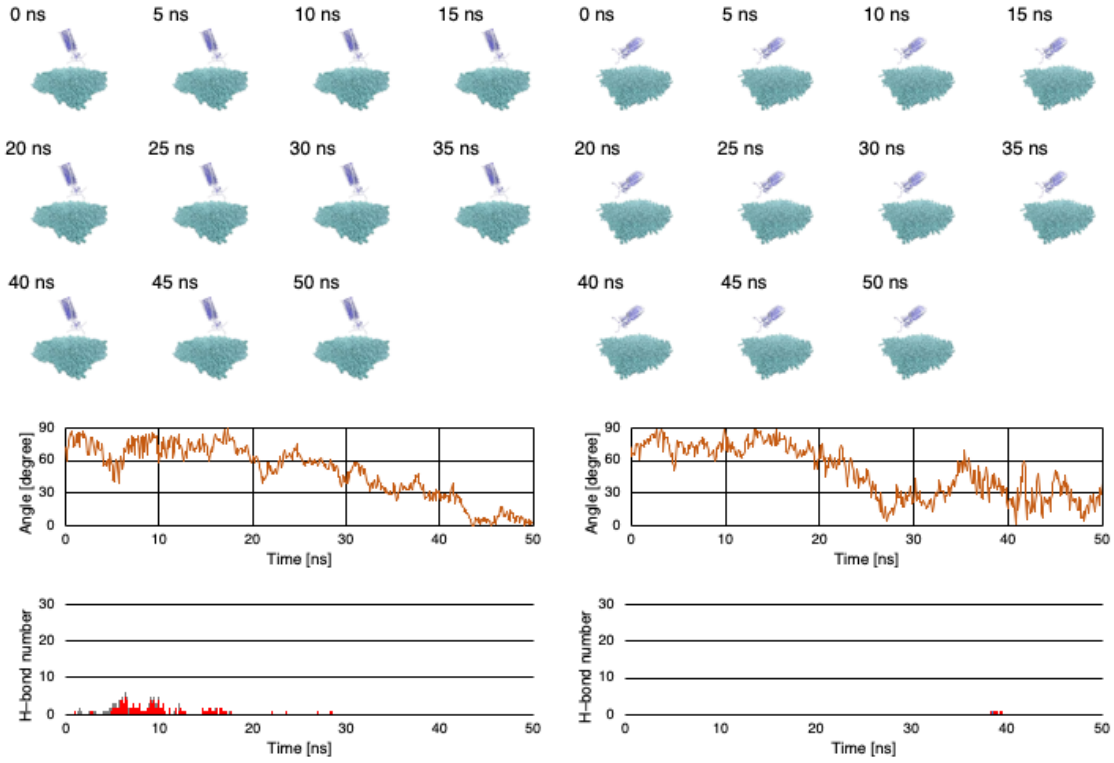

Fig. S4. Two MD simulation results of **PN** with the DOPC membrane with the initial θ_{PN} of 90°. Snapshots of the simulations of **PN**. Time course of number of hydrogen bond between the membrane and **PN**. The number of hydrogen bonds for 50 ns was counted every 0.1 ns. The number of hydrogen bonds between the His-tag fragments and the phosphate group of DOPC was colored with red. All the residues except for the His-tag fragments of **PN** and the phosphate group of DOPC were colored with gray.

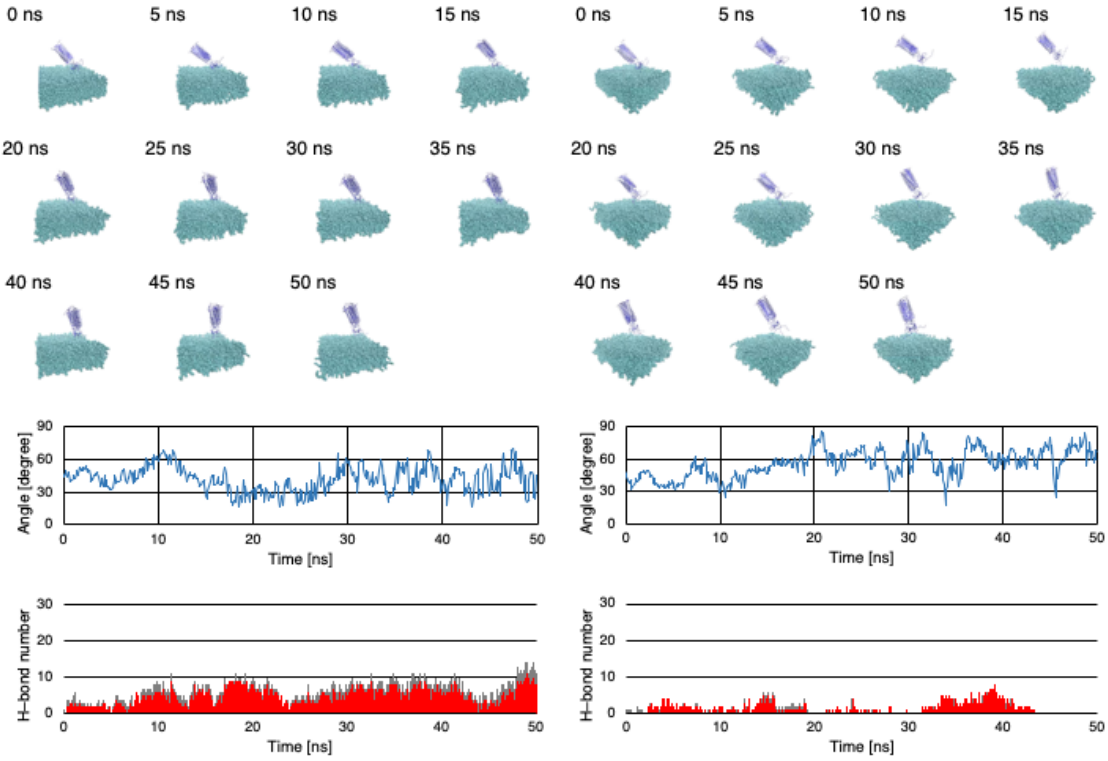

Fig. S5. Two MD simulation results of **PN** with the DOPC membrane with the initial θ_{PN} of 45°. Snapshots of the simulations of **PN**. Time course of number of hydrogen bond between the membrane and **PN**. The number of hydrogen bonds for 50 ns was counted every 0.1 ns. The number of hydrogen bonds between the His-tag fragments and the phosphate group of DOPC was colored with red. All the residues except for the His-tag fragments of **PN** and the phosphate group of DOPC were colored with gray.

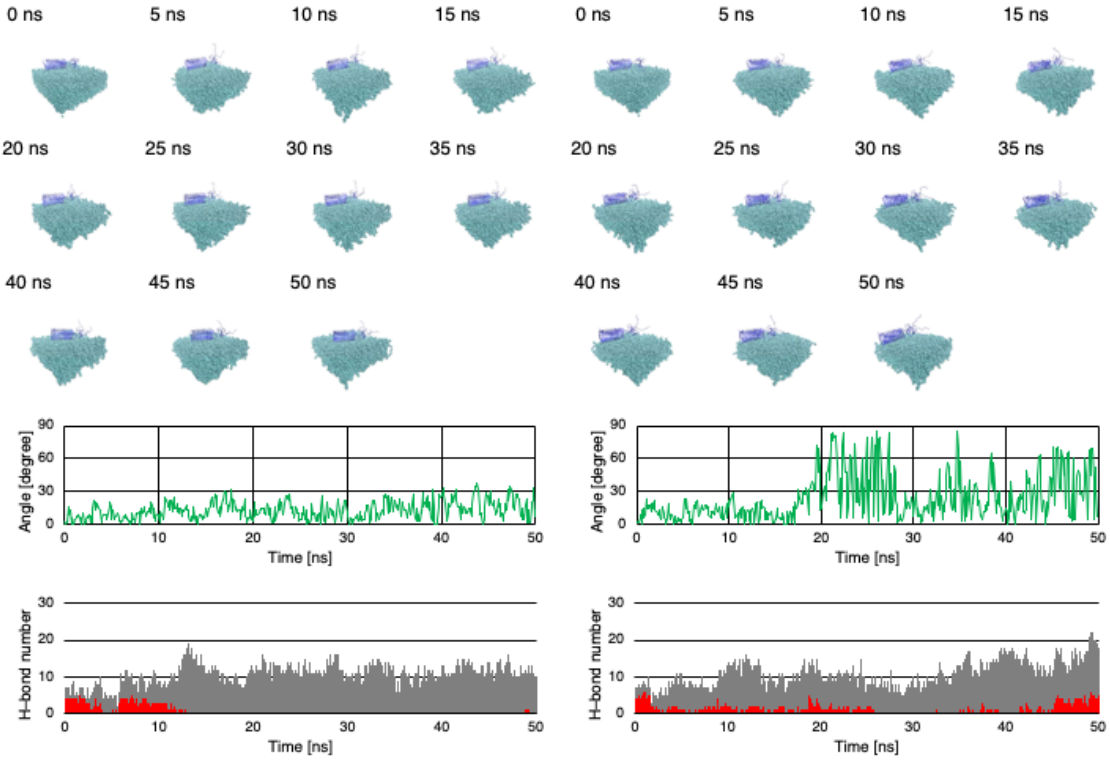

Fig. S6. Two MD simulation results of **PN** with the DOPC membrane with the initial θ_{PN} of 0°. Snapshots of the simulations of **PN**. Time course of number of hydrogen bond between the membrane and **PN**. The number of hydrogen bonds for 50 ns was counted every 0.1 ns. The number of hydrogen bonds between the His-tag fragments and the phosphate group of DOPC was colored with red. All the residues except for the His-tag fragments of **PN** and the phosphate group of DOPC were colored with gray.

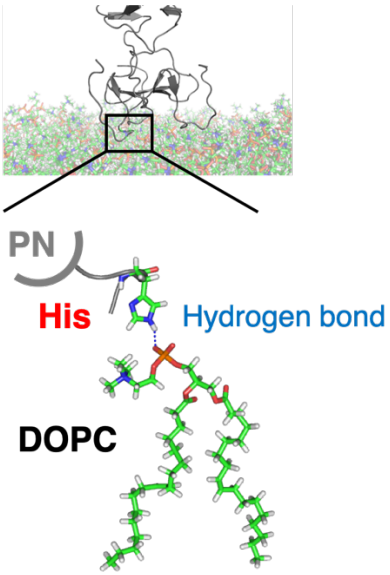

Fig. S7. Represented structure of a hydrogen bond by the His-tag fragment with phosphate group of DOPC. This is a simulation result started with $\theta_{PN} = 45°$.

Movies

Movie S1. HS-AFM movie of **PN** contacting to the DOPC membrane.

Movie S2. HS-AFM movie of **PN_ΔHis** contacting to the DOPC membrane.

Movie S3. MD simulation of **PN** contacting to the DOPC membrane with θ_{PN} of 90°

Movie S4. MD simulation of **PN** contacting to the DOPC membrane with θ_{PN} of 45°

Movie S5. MD simulation of **PN** contacting to the DOPC membrane with θ_{PN} of 0°